Session XI

Thursday, September 8 - morning

C38

EXPERIMENTAL ASSESSMENT OF THE SPATIAL TRANSVERSE DISPLACEMENT OF X-RAYS BY PERFECT CRYSTALS IN VIEW OF SELF-SEEDING APPLICATIONS

A. Rodriguez-Fernandez[1], S. Reiche[1], K. Finkelstein[2], B. Pedrini[1]

[1]Paul Scherrer Institut, CH-5232 Villigen PSI
[2]Cornell University (CHESS), Ithaca, New York
Angel.rodriguez@psi.ch

Free-electron laser (FEL) radiation arises from shot noise in the electron bunch, which is amplified along the undulator section and results in X-ray pulses consisting of many longitudinal modes [1]. The output bandwidth of FELs can be decreased by seeding the FEL process with longitudinally coherent radiation. In the hard X-ray region, there are no suitable external sources. This obstacle can be overcome by self-seeding. The X-ray beam is separated from the electrons using a magnetic chicane, and then monochromatized. The monochromatized X-rays serve as a narrowband seed, after recombination with the electron bunch, along the downstream undulators. This scheme generates longitudinally coherent FEL pulses.

Geloni et al. [2] have proposed monochromatization based on Forward Bragg Diffraction (FBD), which introduces a delay of the narrowband X-rays pulse (echoes) of the order of femtoseconds that can be matched to the delay of the electron bunch due to the chicane. Simulations based in the dynamical diffraction theory show a transverse displacement of the FBD X-ray beam, which can result in a loss of efficiency of the seeding process [3]. The delays and transverse displacements of the echoes are related by

$$x_0 \quad c \cos \qquad (1)$$

where is the Bragg angle of the crystal involved reflection for the average incoming photon energy. Fig. 1 presents the electric field amplitude E_H of the radiation transmitted in the forward direction as a function of transverse position and time on a section downstream a 600 m thick diamond crystal oriented in symmetric (4,0,0) Bragg geometry, and illuminated by a 10 keV beam of 10 m waist size. The two panels correspond to Bragg and Laue, respectively. In both panels, the dependence of the echo transverse displacement on the echo delay expressed in (1) is clearly visible.

To confirm the simulations, an experimental set-up was designed that fulfil the beam characteristics required for this type of studies (small energy bandwidth, beam size of about 10 m and small angular divergence are crucial). For this reason, after a Si (111) monochromator the beam is refined with a channel cut set of Si (531) crystals that reduce the angular width of incoming beam to 1.075'', which is slightly smaller than the expected Darwin acceptance for Diamond (400) Bragg reflection at 10 keV of 1.485''.

The layout of at Cornell High Energy Synchrotron Source (CHESS) C-line Beamline and Material Science (MS) beamline at Swiss Light Source (SLS) is shown in Fig. 2. The beam size was set to 12 ± 2 m by slits located upstream the channel cut set of crystals. A point detector

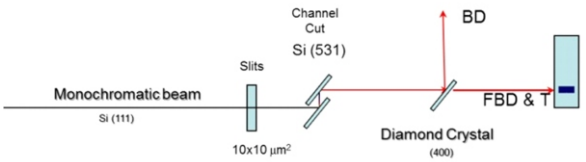

Figure 2. Experimental set-up for the experiment performed at C line at CHESS.

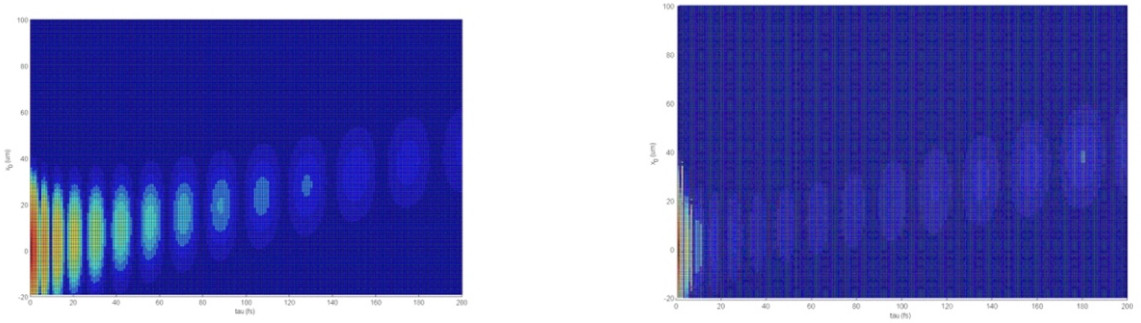

Figure 1. Forward diffracted field magnitude E_H from the (400) Bragg reflection at 10 keV for a 600 m thick Diamond crystal in the case of a 10 m size incident x-ray beam. Calculated following Lindberg and Shvyd ko approximation [3], (Left) Bragg and (right) Laue geometry.

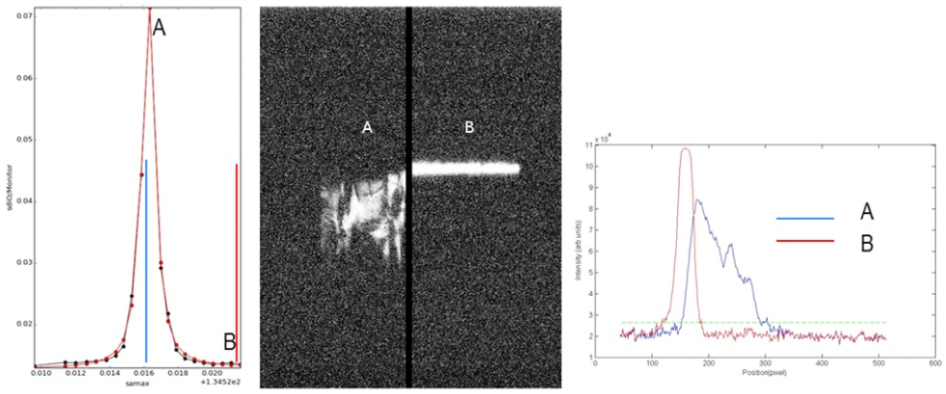

Figure 3. Forward Bragg diffraction signal of a 300 m thick diamond crystal at a 10 keV for the (400) reflection observed at Material Science Beamline of SLS. (Left) Bragg diffraction signal at the BD detector, (Center) signal at the FBD direction detector and (right) section of the FBD detector at two Bragg angles A (in the Bragg condition) and B (far from the Bragg condition).

was situated in the Bragg diffraction direction, 44.04°, which mission was record the width and intensity of the Bragg diffracted signal. The detector in the forward direction uses a GGG scintillator crystal to convert x-ray to visible photons, which are recorded with a high resolution camera with a resolution of less than 2 m/pixel. The samples under study were a series of diamond single crystal with thicknesses between 600 and 100 m. For each scan the sample was set up to the maximum Bragg diffraction signal of the NaI detector at 10 keV, one fixed the channel cut set was rotated allowing just a determined energy to go throw it with high resolution. Recording the signal transmitted thru the crystal in the forward camera.

An example of the data collection results is presented in Fig. 3. It is possible to observe how near the Bragg condition of diffraction, marc in the figure as A, the forward diffracted signal is displaced from the initial position, marc as B, and a series of maxima appear to be formed in the tail of the Bragg peak which are related to the echoes signal.

The results from the experiments performed at CHESS and SLS are beam compare with farther simulations of the beam properties at the synchrotron sources to be able to confirm the predicted transverse displacement, which in the case of a positive confirmation should be taken into account in the design of self-seeding infrastructure for optimizing the FEL performance. In a second step, beamtime at a FEL facility will be requested to correlate the different maxima shown in Fig. 3 with the actual delays.

1. J. S. Wark, et al., J. Apply. Crystallogr. **32**, (1999) 692.
2. G. Geloni, et al. DESY report 10-053 (2010).
3. Y. Shvyd'ko, et al. Phys. Rev. ST Accel. Beams 15, (2012) 100702

The authors acknowledge the staff of the Material Science beamline at Swiss Light Source and of the C-1beamline at Cornell High Energy Synchrotron Source, at which experiments related to this project were performed.

C39

X-RAY BEAM SPLITTING BY USE OF REFLECTION GRATINGS FOR PHOTON ENERGIES OF 4 – 12.4 kEV

W. Jark, D. Eichert

Elettra – Sincrotrone Trieste S.c.p.A., S.S. 14 km 163.5, I-34149 Basovizza (TS),Italy

Recently surprisingly high diffraction efficiencies were observed when a reflection grating was used in the conical diffraction scheme in combination with X-rays with photon energies between 4 and 12.4 keV [1]. As shown in figure 1 the conical diffraction is obtained when the trajectory of the incident beam is parallel to the grooves of the grating. In this case the incident intensity is diffracted into a cone symmetric around the plane of incidence. The highly efficient symmetric diffraction opens the possibility to use such gratings also as optical components for the X-ray range.

An interesting application is as an amplitude beam splitter. Beam splitting with equal intensity cannot only be achieved for two beams but also for more beams. The concept can thus be applied for interferometry experiments or simply for separating a high intensity beam for the use in different experimental stations. We will report related experimental data and compare them to predictions, which will allow us to discuss the optimum parameters for given applications.

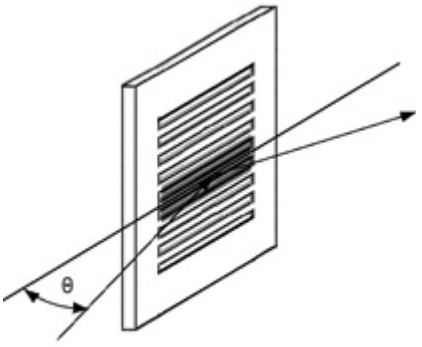

Figure 1. Principal beam trajectory parallel to the grooves when a reflection grating with rectangular groove profile produces conical diffraction in the extreme off-plane configuration for diffraction.

1. W. Jark and D. Eichert, *Opt. Express* **23**, 22753 (2015).

C40

DUAL DETECTOR SINGLE SHOT FAST QUANTITATIVE PHASE MICRO-TOMOGRAPHY

R. Mokso[1], M. Nyvlt[2,3], H. Kohr[4], P. Oberta[5], M. Skeren[2,3], M.Stampanoni[6,7]

[1]Max IV Laboratory, Lund University, SE-22100 Lund, Sweden
[2]FNSPE, Czech Technical University, Czech Republic
[3]Holoplus s.r.o., Prague, Czech Republic
[4]Dpt. Mathematics. KTH Stockholm 10044 Stockholm, Sweden
[5]Rigaku innovative Technologies, Czech Republic
[6]Swiss Light Source, Paul Scherrer Institut, 5232 Villigen PSI, Switzerland
[7]Institute for Biomedical Engineering, University and ETH Zurich, 8092 Zurich, Switzerland
rajmund.mokso@maxiv.lu.se

The first tomographic microscopy beamlines are currently proposed on the diffraction limited storage ring of Max IV. The main emphasis will be on micrometer resolution dynamic studies with high sensitivity to make optimal use of an intense X-ray beam with typically 20-50% coherent fraction and a spot size of 1 mm in diameter will scatter on the sample and give rise to interference fringes recorded in the near field - Fresnel regime. The state-of-the art indirect detector systems for micrometer resolution tomography employs a thin scintillator screen which typically converts about 50% of the X-rays at 20 keV to visible light that is then collected by a lens systems and reaches the detector sensor. We can improve this X-ray photons collection efficiency by using instead a semi transparent scintillator-mirror system and a second detector further downstream of the beam (see Fig. 1a). The added value of such optimization is the simultaneous recording of two distinct Fresnel diffraction patterns [1]. In respect to fast phase imaging the dual-detector principle favours the implementation of quantitative phase retrieval methods requiring data at a minimum of two defocus distances. They are of particular interest if the interaction of a transversely highly coherent X-ray beam scattered on the sample gives rise to multiple and well visible interference fringes in the Fresnel regime. Contrast transfer function based phasing methods [2] can under these conditions deliver optimal results and may therefore be considered for Max IV to complement the often used transport of intensity based phase retrieval [3].

Beside direct phasing methods from two simultaneous projections (Fig. 1b) we have implemented an iterative

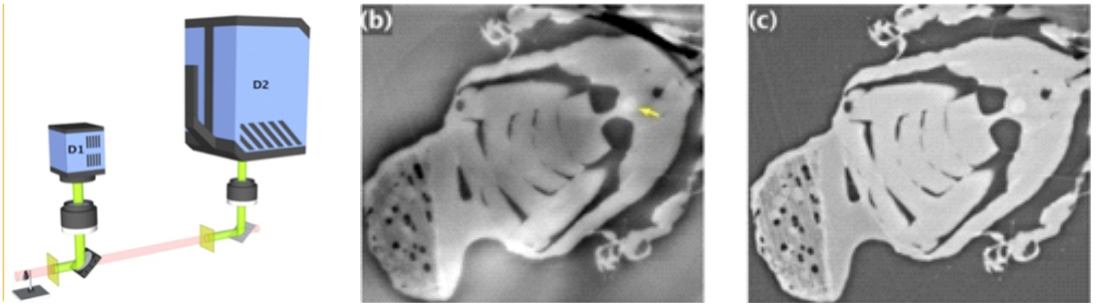

Figure 1. (a) The schematic representation of the dual detector system as implemented at the TOMCAT beamline at the Swiss Light Source. (b) Tomographic slice of a fly thorax reconstructed from the retrieved phase maps using CTF mixed approach based on simultaneously acquired two Fresnel diffraction patterns at sample-to-detector distances set to 4 and 377 mm. The effective pixel size on the first detector D_1 was 2.75 m and it was 2.9 m on the second detector D_2. In (c) a Paganin [3] type reconstruction is shown.

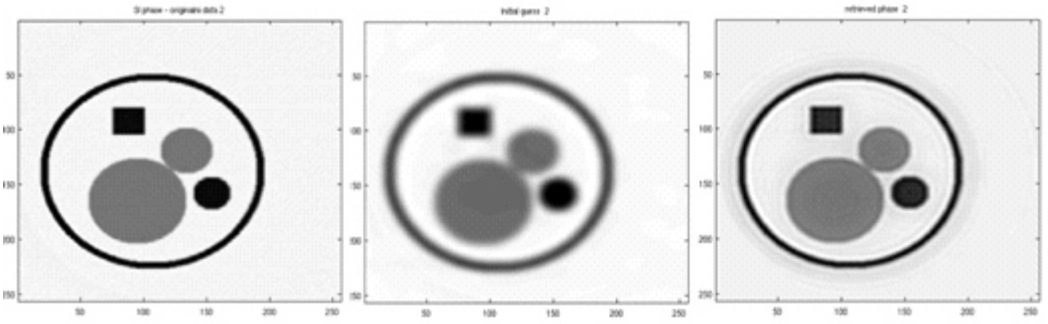

Figure 2. Phase retrieval performed on a phantom. The original tomographic slice of a phase map on the left a Paganin phase retrieval result in the middle and on the right a tomographic slice of resulting from the proposed iterative 3D phase retrieval based on two tomographic sets acquired at various defocus distances.

Fourier transform algorithm interlacing iterations at the phase retrieval and tomographic level. We propose to take advantage of the 3D structure of the recorded diffraction patterns to guide the phase retrieval by the naturally occurring constrains when the full 3D information about the sample is available in two imaging conditions. Furthermore with the proposed scheme we address the problem of background variations during the tomographic acquisition. The performance of this approach is illustrated on Fig 2.

The iterative 3D phase retrieval is being implemented in Operator Discretization Library (ODL) [4], a Python framework for rapid algorithm development in tomography. It offers the possibility to apply a variety of solver schemes to a particular reconstruction problem, for example the conjugate gradient method or TV regularization [5]. In particular, the full non-linear problem of phase tomography can be addressed without any linearization or model simplification. We will present the newest results based on the optimized iterative scheme and discuss the advantages of the small and highly coherent beam at Max IV to pursue high resolution phase tomographic studies in particular for bio-medical applications [6,7]. Some approaches will be built upon the experience gained from pilot studies performed at the TOMCAT beamline at the Swiss Light Source.

Simultaneous acquisition of two Fresnel diffraction patterns may be achieved also by using a crystal beam splitter as theoretically proposed in [8] and experimentally demonstrated in [9]. Of particular interest in this approach is that wavelength separation of the two beams is possible and therefore we can fine-tune the information content in each diffraction pattern independently.

1. R. Mokso, F. Marone, S. C. Irvine, M. Nyvlt, D. Schwyn, K. Mader, G. K. Taylor, H. G. Krapp, M. Skeren, M. Stampanoni, *J. Phys. D. Appl. Phys.* **46**, (2013), 494004.
2. P. Cloetens, W. Ludwig, J. Baruchel et al. *Appl. Phys. Lett.,* **75**, (1999), 2912-1914.
3. D. Paganin, S.C. Mayo, T.E. Gureyev et al. *J. Microscopy* **206**, (2002), 33-40.
4. https://www.github.com/odlgroup/odl
5. V. Caselles, A. Chambolle, M. Novaga. *Handbook of Mathematical Methods in Imaging* (2011), 1016–1057.
6. R. Mokso, D. A. Schwyn, S. M. Walker, M. Wicklein, T. Müller, M. Doube, M. Stampanoni, G. K. Taylor, H. G. Krapp, *Scientific Reports* **5**, (2015), 8727.
7. G. Lovric, S. F. Barré, J. C. Schittny, M. Roth-Kleiner, M. Stampanoni, R. Mokso, *J. Appl. Crystallogr*. **46**(4), (2013), 856.
8. P. Oberta & R. Mokso, A Laue-bragg monolithic beam splitter for efficient x-ray 2-beam imaging. *Nucl. Inst. Meth.* **703**, (2013), 59–63.
9. R. Mokso & P. Oberta, Simultaneous dual-energy X-ray stereo imaging. *J. Synch. Rad.* **22**(4), (2015), 1078-82.

C41

X-RAY IMAGING AT THE ADVANCED PHOTON SOURCE: OPPORTUNITIES WITH THE APS UPGRADE

Francesco De Carlo, Kamel Fezzaa, Vincent De Andrade, Tao Sun, Xianghui Xiao, Xiaogang Yang and Doga Gürsoy

Argonne National Laboratory, 9700 S. Cass Av. Argonne IL 60439
decarlo@aps.anl.gov

Full-field imaging is an extremely versatile technique that is broadly applicable to almost all scientific and engineering disciplines. Its versatility is reflected by the fact that every major synchrotron facility in the world has a dedicated full-field imaging facility. In many cases, full-field imaging is the keystone linking a sample to other X-ray techniques such as ptychography, μXRF, μXANES, and μXRD.

The current Advanced Photon Source (APS) allows for hierarchical 3D imaging of dynamic systems and materials with spatial resolution up to 1μm, without a major sacrifice in time resolution and 20 nm 3D imaging of static or slowly evolving systems.

In this talk we will present the latest nano and dynamic imaging results utilizing the current APS source and will describe the opportunities the new APS upgrade source will bring to this technique.

This research used resources of the Advanced Photon Source, a U.S. Department of Energy (DOE) Office of Science User Facility operated for the DOE Office of Science by Argonne National Laboratory under Contract No. DE-AC02-06CH11357.

1. J.W. Gibbs, K.A. Mohan, E.B. Gulsoy, A.J. Shahani, X. Xiao, C.A. Bouman, M. De Graef, P.W. Voorhees, "The Three-Dimensional Morphology of Growing Dendrites," *Sci. Rep.* **5**, 11824-1-11824-9 (2015). DOI: 10.1038/srep11824.

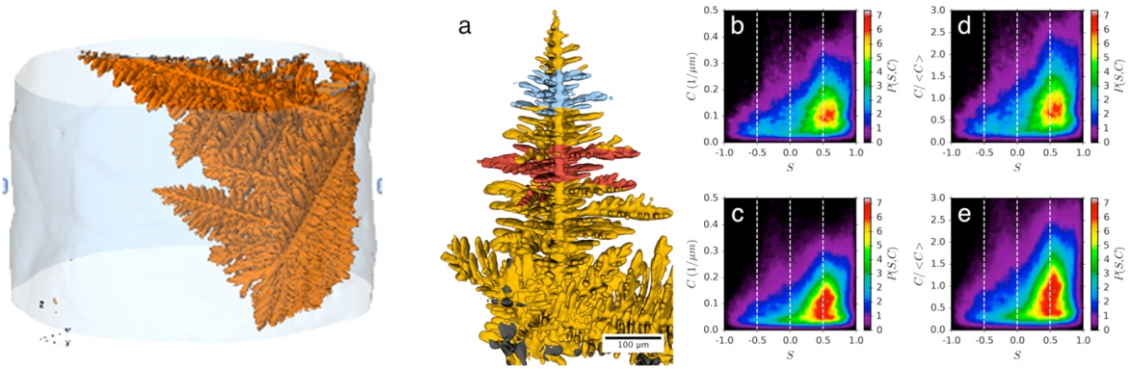

Figure 1. Left: animation at 1.6 3D-fps growth of Al-rich dendrite in Al-Cu alloy with a cooling rate 1 K/min from 550 K. Right: Interfacial shape distributions for two 75 m thick slices normal to the growth direction of the nearly free-growing dendrite at 9.0 seconds after nucleation [1].